JOURNAL OF STRUCTURAL BIOLOGY **115,** 68–77 (1995)

Electron Microscopy of the GroEL–GroES Filament

J. R. HARRIS

Institute of Zoology, University of Mainz, Mainz, Germany

R. ZAHN[1]

Max-Planck-Institute for Biochemistry, Martinsried, Germany

AND

A. PLÜCKTHUN

Institute of Biochemistry, University of Zürich, Zürich, Switzerland

Received April 7, 1995, and in revised form June 18, 1995

Electron microscopy of a filamentous complex of GroEL and GroES has been performed on negatively stained specimens. The filaments have been formed when GroEL and GroES at relatively low molar ratios (e.g., 1:1 to 1:3) are incubated at room temperature in the presence of magnesium and ATP. At higher molar ratio, the symmetrical GroEL–GroES complex predominates. Within the GroEL–GroES filaments, the same structural rearrangements of GroEL were observed as in the "bullet-shaped" or symmetrical GroEL–GroES complexes. In the absence of GroES, GroEL molecules have no tendency to form linear filaments. The sharing of one GroES by two GroEL molecules might indicate a high plasticity of the GroEL–GroES complex. Preliminary Fourier analysis of filaments of increasing length indicates that they possess an inherent helicity. Using the negative staining-carbon film procedure, two-dimensional (2-D) crystal nucleation induced by ammonium molybdate-polyethylene glycol can create undulatory rows of side-on GroEL molecules, which are able extend as a p2 2-D crystal form, readily distinguishable from the filamentous GroEL–GroES aggregates. Crystallographic image processing indicates that the GroEL 2 × 7-mer itself possesses a dyad screw axis, in accord with existing higher resolution X-ray structure data. © 1995 Academic Press, Inc.

[1] Present address: MRC Unit for Protein Function and Design, University Chemical Laboratory, Lensfield Road, Cambridge, UK.

INTRODUCTION

Interest in protein folding in general and in the function of molecular chaperones in particular has extended significantly in recent years (Gething and Sambrook, 1992; Martin *et al.,* 1993; Hendrick and Hartl, 1993). Determination of the structure of *Escherichia coli* GroEL (cpn60/hsp60) at 2.8 Å by X-ray crystallography (Braig *et al.,* 1994) has provided a major advance in structural insight into this chaperone and now enables correlation with the electron microscopical structural data on GroEL to be made.

The crystallographic analysis of GroEL confirms the hollow cylindrical shape, constructed from two rings containing seven 60-kDa subunits stacked with dyad symmetry. The subunits contain three domains with the largest, the equatorial domain, responsible for the construction of each heptameric ring and for the central intersubunit contacts between the two stacked rings in the native molecule. A 25.7° rotation between the two rings occurs at the equatorial plane, creating dyad symmetry from the two asymmetrical 7-mer units. The end regions of the cylinder are constructed by the apical polypeptide-binding domains of the subunits, which are linked to the equatorial nucleotide-binding domain by a smaller intermediate domain. This intermediate domain is interspaced by seven elliptical side windows, thereby creating a zone containing a lower mass thickness of protein. This detailed high-resolution description of the subunit domains and their location within the intact 2 × 7-mer (Braig *et al.,* 1994) correlates well with the 2-D projection images from negatively stained specimens of GroEL and

1047-8477/95 $12.00

other cpn60 oligomers (Zwickl *et al.,* 1990; Zahn *et al.,* 1993; Harris *et al.,* 1994) and images from unstained frozen-hydrated GroEL (Chen *et al.,* 1994). The principal zones/rings of protein thickness conform with the equatorial and apical subunit domains within both negatively stained and unstained vitrified images.

GroEL has been shown to bind unfolded polypeptide substrates by hydrophobic interactions (Fenton *et al.,* 1994; Zahn and Plückthun, 1994; Zahn *et al.,* 1994b). Upon binding, the complete tertiary and secondary structure is considerably destabilized (Zahn *et al.,* 1994a; Robinson *et al.,* 1994). Only stable intermediates can dissociate from GroEL, thereby preventing irreversible protein aggregation reactions (Buchner *et al.,* 1991; Zahn and Plückthun, 1992). For release of the bound polypeptide and subsequent folding, many substrate proteins require the participation of GroES and/or ATP (Goloubinoff *et al.,* 1989; Laminet *et al.,* 1990). The X-ray structure of GroES has not yet been determined, but from biochemical and electron microscopical data GroES appears to be a ring-like molecule, possibly also possessing sevenfold rotational symmetry (Chandrasekhar *et al.,* 1986; Harris *et al.,* 1994).

Claims that the GroEL–GroES complex contains GroEL and GroES in a strictly 1:1 molar ratio (2 × 7-mer:1 × 7-mer), thereby creating a "bullet-shaped" complex (Ishii *et al.,* 1992; Saibil *et al.,* 1991, 1993; Langer *et al.,* 1992) have been reinvestigated following the detection of an ellipsoidal form. This symmetrical structure, which appears to form under conditions used for protein folding experiments, probably contains a heptamer of GroES bound at both ends of the GroEL cylinder (Azem *et al.,* 1994; Harris and Horne, 1994; Harris *et al.,* 1994; Lorca *et al.,* 1994; Schmidt *et al.,* 1994; Todd *et al.,* 1994). The exact conditions for symmetrical GroEL–GroES complex preparation vary somewhat from laboratory to laboratory, but it is now clear that it requires a sufficient excess of GroES to be present, along with magnesium and ATP, and that the incubation be performed at room temperature for a period of many minutes or hours rather than a few seconds.

We have also shown that at low molar ratios of GroES:EL (i.e., 1:1 to 3:1) and short times of incubation the interaction does indeed promote the formation of the bullet-shaped GroEL–GroES complex and filamentous aggregates are also formed over a period of hours (Harris *et al.,* 1994). We present here further structural analysis of the linear aggregates of GroEL and GroES and show that they are clearly distinguishable from the undulatory rows of side-on GroEL molecules in disordered two-dimensional (2-D) arrays and 2-D crystals.

MATERIALS AND METHODS

Chemicals

Biochemical reagents were routinely purchased from the Sigma Aldrich Vertriebs GmbH (Diesenhofen). Electron microscopical materials and reagents were purchased from Plano (W. Plannet GmbH), Marburg, Germany.

Purification of GroEL and GroES

GroEL and GroES were purified from *Escherichia coli* strain W3110, containing the plasmid pOF39, as previously described (Harris *et al.,* 1994). Protein concentrations were determined following amino acid analysis. The ratio of GroEL to GroES is always given for the oligomeric proteins.

Formation of GroEL–GroES Filamentous Complexes

Complexes of GroEL and GroES were prepared as previously described by Harris *et al.* (1994). Briefly, aliquots of purified GroEL (1 mg/ml: ca. 1.2 μM) and GroES were mixed in known molar ratios (1:1, 1:2, 1:3, 1:4, and 1:10) in 5 mM Tris–HCl buffer (pH 8.0) containing 1 mM ATP and 2 mM $MgCl_2$ and incubated at room temperature for time periods extending up to 2 days. Most studies on the filamentous GroEL–GroES complexes were carried out at the two lower molar ratios, and samples were taken for specimen preparation by conventional negative staining with uranyl acetate at time periods of 1 and 2 hr after mixing.

Preparation of Negatively Stained Specimens

Negatively stained specimens were prepared by the single droplet procedure (Harris and Horne, 1991) using carbon films that had been treated for 20 sec by glow discharge in a partial atmosphere, to render them hydrophilic and adsorptive. Routinely, 2% aqueous uranyl acetate containing 0.1% octylglucoside to improve spreading and stain penetration (Harris and Horne, 1994) was used, although some studies were performed using 4% uranyl acetate containing 1% trehalose.

Formation of 2-D Arrays and 2-D Crystals of GroEL on Mica

The preparation of 2-D arrays and 2-D crystals of GroEL was performed on mica using the negative staining-carbon film procedure (Horne and Pasquali-Ronchetti, 1974), in the presence of both ammonium molybdate and polyethylene glycol, as previously described (Zahn *et al.,* 1993; Harris *et al.,* 1994). After carbon coating and removal of the layer of carbon plus adsorbed protein, the negative stain was 2% uranyl acetate containing 0.1% octylglucoside (Harris and Horne, 1994).

Electron Microscopy

Transmission electron microscopy was performed using the Zeiss EM 900 and the Jeol 120EX electron microscopes under conventional yet minimal bright-field illumination conditions. Low-temperature studies were performed at −175°C, using the Philips EM400 electron microscope with a Gatan cryoholder. Electron micrographs were recorded on Kodak type 4489 and SO-163 and AGFA 23D56 EM film at instrumental magnifications between ×30000 and ×85000. Magnifications were calibrated using thin crystals of bovine liver catalase (Wrigley, 1968).

Image Processing

Power spectra of the filamentous GroEL–GroES aggregates were produced from filaments individually cut from electron micrographs, using the CRISP software system. Helical image reconstruction was not possible using this software. Crystallo-

graphic analysis of the 2-D crystals of GroEL was performed using the full application of the CRISP system (Hovmöller, 1992), which selected a p2 plane group symmetry for the crystal form under study (Harris *et al.,* 1994).

RESULTS AND DISCUSSION

At a 1:1 or 3:1 molar ratio of GroES:GroEL (22°C in the presence of 1 m*M* ATP and 2 m*M* $MgCl_2$) the oligomeric proteins form filamentous complexes over a period of hours and ultimately yield large paracrystalline precipitates (Harris *et al.,* 1994). At shorter incubation times (e.g., 1 or 2 hr) the specimens prepared were found to contain individual filaments of varying length (Fig. 1), as well as small paracrystalline aggregates (see below). Although the time required for this macromolecular interaction might seem to be rather long, it is similar to tubulin polymerization into microtubules and is significantly shorter than the times required to produce reassociation of dissociated keyhole limpet hemocyanin (Harris *et al.,* 1995). Most of the filaments have curved ends, characteristic of the ends of the ca. 24-nm symmetrical GroEL–GroES complex or the single curved end of the ca. 20-nm bullet-shaped complex (compare Figs. 1 and 2). Occasionally, a blunt-ended filament can be detected, probably due to the absence of a terminally bound GroES molecule. It also appears likely that the terminal GroEL molecules may sometimes split equatorially (see arrowheads, Fig. 1), with one of the pronounced equatorial domain rings of the GroEL then exposed at the end of a filament. Such splitting of the GroEL 2 × 7-mer

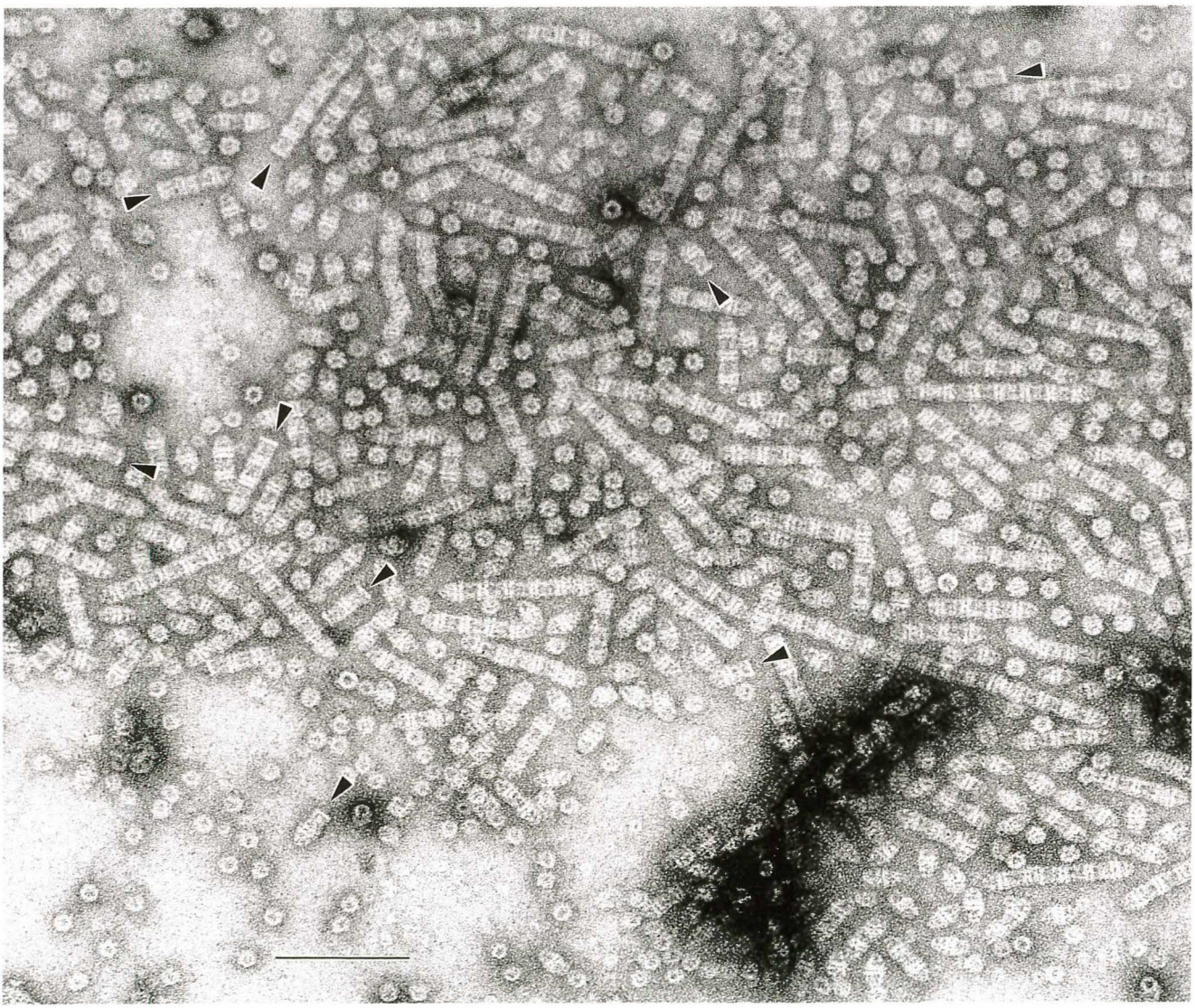

FIG. 1. A survey electron micrograph showing negatively stained GroEL–GroES filamentous complexes of varying length, prepared with a molar ratio of ca. 1:3 GroEL:GroES. Negatively stained with 2% uranyl acetate containing 0.1% octylglucoside. Arrowheads indicate filaments that appear to terminate by equatorial splitting of a GroEL molecule. Scale bar, 100 nm.

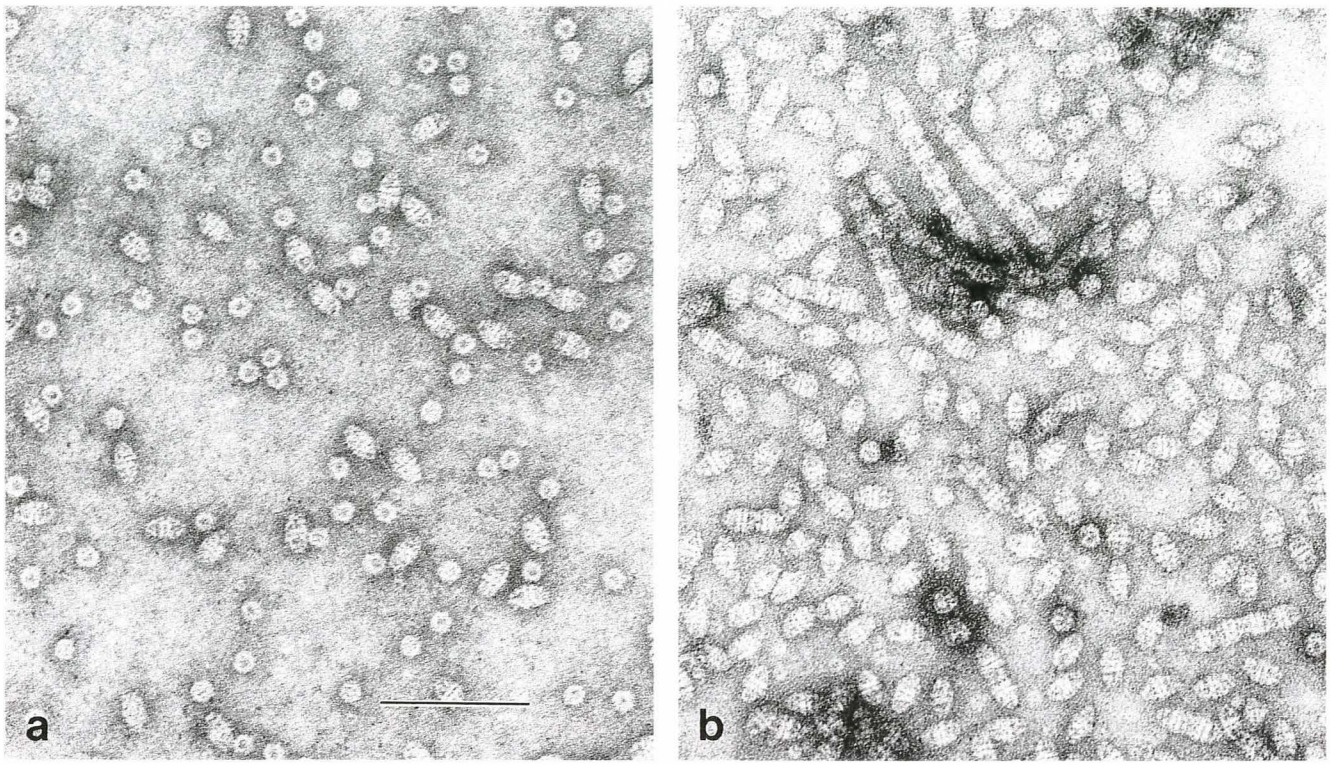

FIG. 2. A survey electron micrograph showing numerous examples of the symmetrical GroEL–GroES complex, mean length ca. 24 nm: (a) (molar ratio GroEL:GroES 1:10) (see also Harris *et al.,* 1994) which in (b) (molar ratio GroEL:GroES ca. 1:4) lie alongside some filamentous GroEL–GroES complexes (cf. Figs. 1 and 3). Note the presence of a considerable number of the ring-like images in (a), fewer in (b). These almost certainly represent vertically positioned symmetrical complexes rather than unreacted GroEL or single-ended "bullet-shaped" complexes, since there is no indication of any rectangular side-on unreacted GroEL molecules (length ca. 15 nm; Braig *et al.,* 1994) or any side-on bullet-shaped complexes. In both cases free GroES can be detected alongside the complexes. Negatively stained with 2% uranyl acetate containing 0.1% octylglucoside. Scale bar, 100 nm.

into single 7-mers has occasionally been observed during the production of 2-D crystals of GroEL (J. R. H., unpublished observations), and indeed it is known that native mitochondrial cpn60 exists as a functional 1 × 7-mer (Viitanen *et al.,* 1992).

A gallery of filaments of increasing length is shown in Fig. 3a, together with three short clusters of parallel filaments. Larger clusters are nearly always rather intensely stained, which prevents satisfactory imaging of their filaments. The power spectra of GroEL–ES filaments containing 4 and 11 GroEL molecules and a short paracrystalline cluster are shown in Figs. 3b, 3c, and 3d, respectively. Preliminary inspection of these power spectra indicates that they possess oblique layer lines, characteristic of helical structures (Stewart, 1986), and all possess strong meridional reflections generated by the ca. 18-nm repeat along the filaments. Characteristic of all negative stained specimens, superimposition of image features from the top and bottom of the filaments is to be expected, possibly combined with uneven or varying depth negative staining. More detailed analysis of these power spectra, together with 2-D and 3-D image reconstruction, is planned for the near future.

From the occurrence of the filaments at low GroES:GroEL ratios, we propose that a single GroES molecule provides a link between adjacent GroEL molecules within the filaments. Although the possibility that two GroES molecules might provide the link cannot be dismissed, it is unlikely from stoichiometric considerations and there is no evidence for dimerization of GroES (i.e., two 10-kDa 7-mers). The large "cavity" within GroEL created by the conformational change following the interaction with GroES (Chen *et al.,* 1994; Langer *et al.,* 1992) is also a repeating feature along the linear filaments, as are the paired equatorial GroEL domains. The interaction between GroEL and GroES within the GroEL–GroES repeating units in the filaments appears to be similar to the specific binding of GroES to the GroES binding sites of the single GroEL molecule. However, the "outside" of GroES on the bullet-shaped GroES–GroEL complex may bind to the available polypeptide binding site at the other end of a similar bullet-shaped GroEL–GroES, thus polymerizing the complex. Reduction of a ca. 20-nm length of the bullet-shaped GroEL–GroES complex to generate the ca. 18-nm periodicity within the filaments is compatible with this model. Thus, the

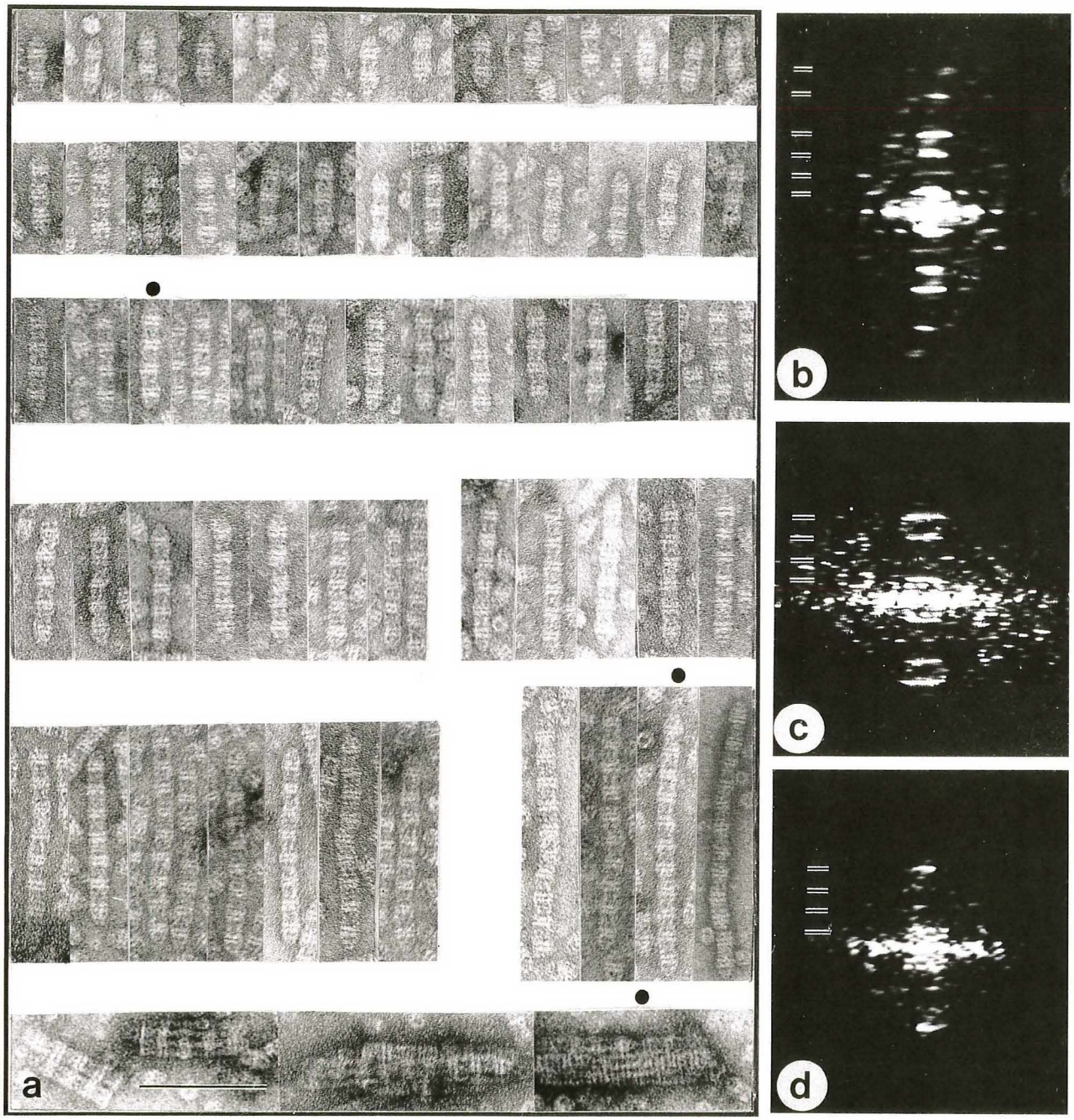

FIG. 3. (a) A gallery of GroEL–GroES filaments (prepared from a 1:3 molar ratio of GroEL:GroES) of increasing length, extracted from electron micrograph regions equivalent to that shown in Fig. 1, together with small parallel clusters of filaments. The linear repeat within the filaments of the GroEL equatorial plane is ca. 18 nm. Scale bar, 100 nm. (b, c, and d) Power spectra of linear GroEL–ES filaments containing 4 and 11 GroEL molecules and a small parallel cluster, respectively, from the individual images indicated (•). The strong (18 nm^{-1}) meridional layer lines are indicated (cf. Fig. 5e).

presence of bound polypeptide substrate within the GroEL molecules may prevent filament formation. This we propose to investigate by the addition of citrate synthase before and after filament formation. Furthermore, addition of excess GroES to the filaments may produce dissociation into symmetrical complexes.

Direct visualization of the GroES molecules in the filaments is not possible at the level of resolution provided by conventional negative staining (ca. 2 nm). Indeed, clear definition of the 70-kDa GroES alone by negative staining is not technically easy (Harris *et al.,* 1994) and has not as yet provided unequivocal confirmation of a "simple" heptameric

ring structure. Direct immunolabeling of GroES within the filaments is a possibility for the localization of GroES (cf. Harris *et al.,* 1993), but we have not pursued this approach to date, and GroES epitopes might not necessarily be accessible to monoclonal antibodies when incorporated within the filaments. It should be noted that the GroEL–GroES filaments we have created are readily distinguishable from the linear chains of antibody-linked *Bordetella pertussis* cpn60 (Cejka *et al.,* 1993) and the smaller immune complexes of GroEL produced by Martin *et al.* (1994).

It is clear that the linear interaction and periodicity of consecutive GroEL molecules within the GroEL–GroES chains is significantly different from that occurring during the nucleation and 2-D crystallization of the GroEL molecules in their side-on orientation on mica (Fig. 4). Here it is shown that within the rows, the GroEL molecules are more closely spaced (linear repeat ca. 15 nm) and undulate with respect to one another, undoubtedly as a means of specifically incorporating a cylindrical molecule with sevenfold rotational symmetry within an ordered monomolecular layer. When extended to the more highly ordered p2 side-on 2-D crystal of GroEL (Fig. 5a), this undulatory feature remains (see below; cf. Harris *et al.,* 1994, Fig. 3), with the longitudinal space between successive individual GroEL molecules more clearly defined than is the case within the linear GroEL–GroES filaments. Nevertheless, since our one-dimensional arrays of GroEL were produced on mica by the negative staining-carbon film technique, the possible production of a more strictly linear one-dimensional polymerization of GroEL molecules by other approaches cannot be dismissed, but this remains to be demonstrated.

As mentioned above, the power spectra of the GroEL–GroES filaments shown in Fig. 3 strongly indicate that the filaments of GroEL and GroES possess a helical symmetry, a feature also detectable within the GroEL 2 × 7-mer alone. Indeed, within the GroEL 2 × 7-mer, the equatorial domains from each of the two asymmetrical 7-mer units are rotated by 25.7° at the central plane (Braig *et al.,* 1994), thereby creating the dyad symmetry and a screw axis. However, the GroEL arrays shown in Figs. 4 and 5a do not contain long filaments, but individual molecules, and they do not show any continuous helical feature. Any longitudinal/axial deviation from linearity of the subunit domains within each GroEL 7-mer, as indicated from the subunit shape and oblique angle within the cylinder wall

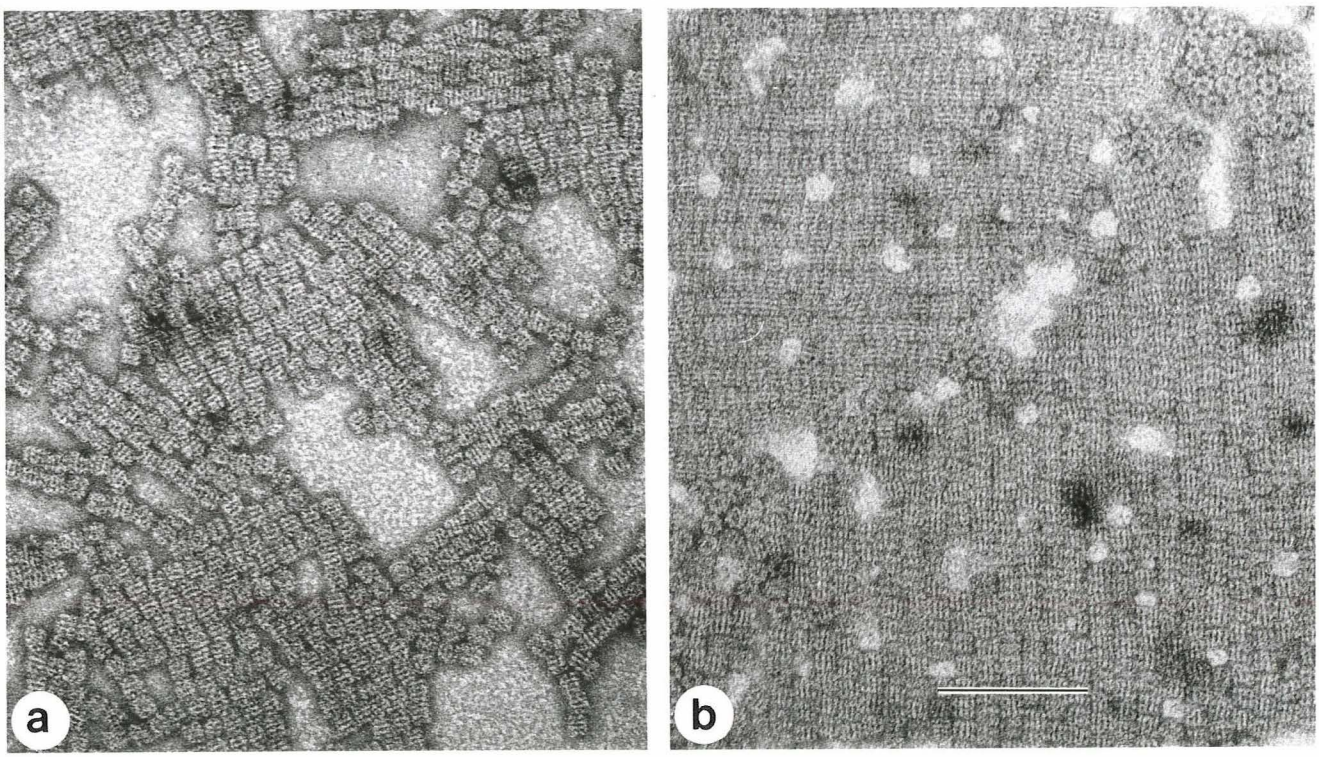

FIG. 4. The nucleation of 2-D crystals of GroEL in the side-on molecular orientation on mica (a) and the creation of incomplete 2-D crystals (b), by the negative staining-carbon film technique. The flexible/undulatory linear chains of molecules (ca. 15-nm repeat) are clearly different from those shown within the GroEL–GroES filaments (Figs. 1 and 3). Negatively stained with 2% uranyl acetate. Scale bar, 100 nm.

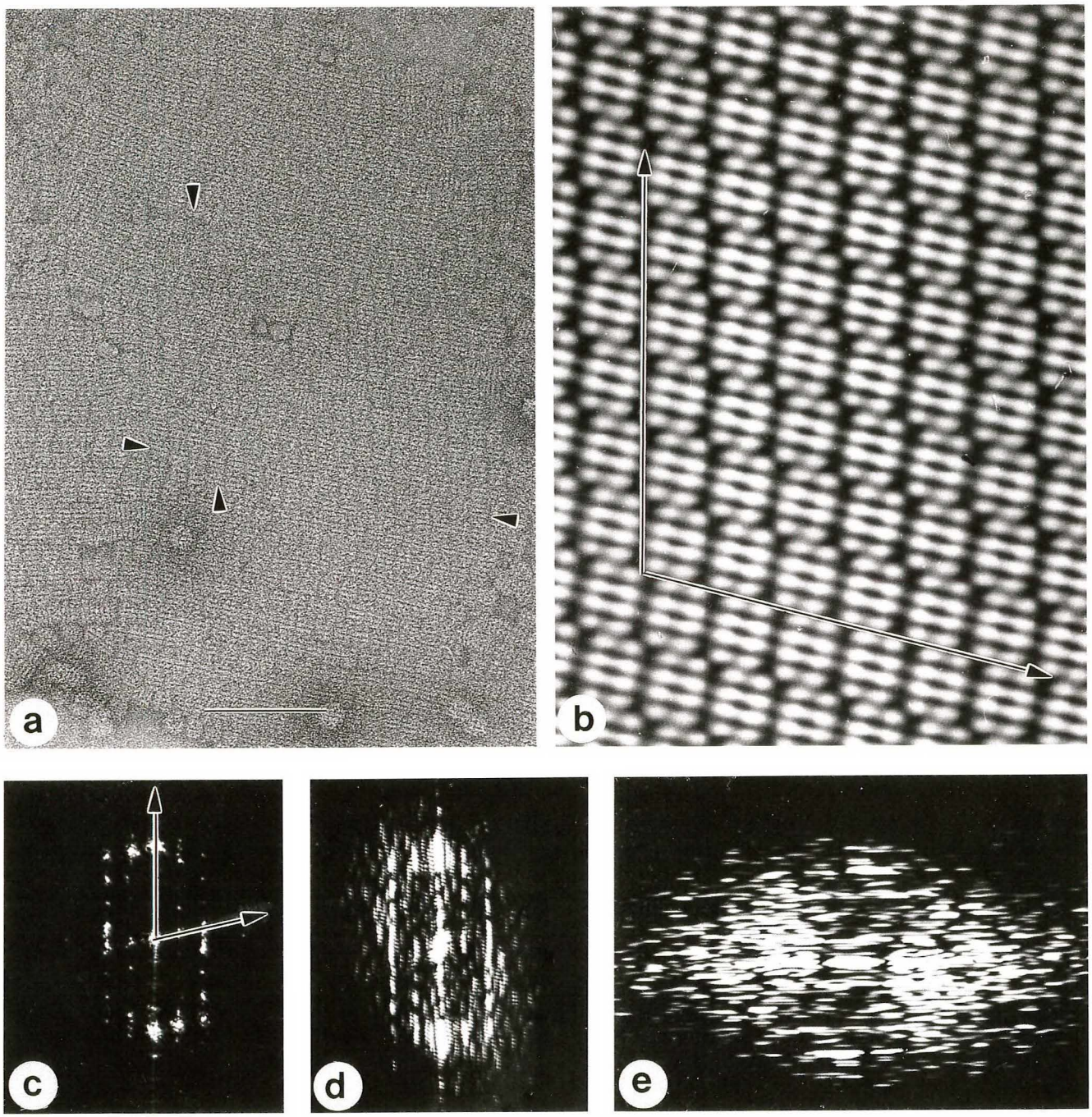

FIG. 5. (a) A well-ordered 2-D crystal of GroEL with molecules in the side-on orientation, negatively stained with 2% uranyl acetate (cf. Harris *et al.,* 1994, Fig. 3; this p2 2-D crystal has shallower negative stain than the one shown here). (b) The p2 crystallographic image reconstruction of the 2-D crystal (phase residual 9.3°). There is one molecule per unit cell, with $\alpha = 15$ nm, $\beta = 14$ nm, and $\beta = 103°$. Note the zig-zag linearity of the rows of molecules within the crystal and compare with the rows of molecules and small 2-D arrays in Fig. 4. (c) The indexed power spectrum from an undistorted part of the p2 2-D crystal in (a). (d and e) The power spectra from single rows of side-to-side molecules (d) and end-to-end molecules (e) (note, this power spectrum is rotated by 90°) within the 2-D crystal shown in (a), as indicated by the paired arrowheads. Note the lack of clarity of the ca. (15 nm^{-1}) layer lines (d and e) and compare with those in the power spectra of the GroEL–ES filaments shown in Figs. 3b–3d. Scale bar (a), 100 nm.

(Braig *et al.,* 1994), could further enhance this inherent helicity. This feature is indeed suggested by the 3-D image reconstruction of negatively stained *Rhodobacter sphaeroids* cpn60 shown by Saibil *et al.* (1993), yet is not apparent in the more recent unstained GroEL 3-D reconstruction from vitreous ice (Chen *et al.,* 1994). Comparison of the six major eigenvector–eigenvalue side-on 2-D projection aver-

ages of the *Comamonas acidovorans* cpn60 (Zwickl *et al.,* 1990) also suggest that the subunits of the molecule possess domains arranged at an angle relative to the sevenfold axis. A preliminary 3-D reconstruction of GroEL from a p2 2-D crystal tilt series (Zahn, 1994; data not shown), which is not considered to be satisfactory due primarily to partial-depth negative staining, also indicates this oblique domain organization. The p2 side-on 2-D crystal of GroEL shown in Fig 5a possesses a somewhat greater depth of negative stain than that of an equivalent 2-D crystal presented by Harris *et al.,* (1994). The 2-D image reconstruction from this p2 crystal (Fig. 5b) indicates more clearly the dyad symmetry of the molecule, as well as the zig-zag/undulatory nature of the end-to-end rows of molecules, in agreement with those participating in 2-D crystal formation, as shown in Fig. 4. Power spectra for the 2-D crystal shown in Fig. 5a together with single rows of side-by-side and end-to-end GroEL molecules are given in Figs. 5b, 5c, and 5d, respectively. The power spectrum of the end-to-end GroEL molecules (Fig. 5d) is particularly noisy, but can still be seen to be significantly different from those of the filamentous GroEL–ES complexes shown in Figs. 3b–3d, in accord with our overall visual interpretations made directly from the negatively stained electron microscopical images.

It is pertinent that a helical molecular conformation is known to exist within the cylindrical molluscan hemocyanins (Mellema and Klug, 1972; Gebauer *et al.,* 1994; Harris *et al.,* 1993). This hemocyanin often exhibits a stable dimeric form, as the ca. 8-mDa didecamer with the decamer is the asymmetrical unit, as well as an asymmetrically stacked-disc multidecameric form (Gebauer *et al.,* 1994; Harris *et al.,* 1993). Molluscan hemocyanins can also generate a continuous (helical) tubular form (Mellema and Klug, 1972; Harris *et al.,* 1995), either following limited proteolysis or during *in vitro* subunit reassociation. In addition to the well-known examples of microtubules and TMV, several other well-characterized macromolecules are known to be able to create helical filamentous and tubular structures, such as sickle cell hemoglobin (McDade and Josephs, 1993), α2-macroglobulin (Couture-Tosi *et al.,* 1986), catalase (Kiselev *et al.,* 1967), glutamate dehydrogenase (Munn, 1972; Josephs and Borisy, 1972), glutamine synthetase (Frey, 1978), and creatine kinase (Schnyder *et al.,* 1994). The salient comparative feature in most of these examples is that filament or tubule formation occurs by linear homooligomerization rather than heterooligomerization, as would appear to be the case within the GroEL–GroES filaments. However, microtubules are constructed from equal amounts of α and β tubulin, and they have the property of being able to bind microtubule-associated proteins (MAPs) and dynein.

The apparent plasticity of the peripheral domains of the GroEL molecule during 2-D crystallization (Zahn *et al.,* 1993) and when interacting with substrate proteins and GroES (Chen *et al.,* 1994; Langer *et al.,* 1992; Saibil *et al.,* 1993), a feature also indicated strongly by the crystal structure (Braig *et al.,* 1994), may explain the ability of two GroEL molecules to be linked by a single GroES molecule. This phenomenon does, nevertheless, remain difficult to explain dynamically and stoichiometrically, following the observation that the binding of the first GroES molecule by GroEL has a stronger interaction than the binding of the second GroES at the opposite end (Todd *et al.,* 1994). In addition, it is generally envisaged that the 70-kDa ring-like GroES itself possesses top to bottom asymmetry, with only one side of the ring able to bind to GroEL in the "conventional" way. GroES would only be able to provide an inter-GroEL link if the interaction to the neighboring GroEL ring is different. The fact that GroES possesses the ability to link GroEL molecules, under conditions of limited GroES availability and slightly extended time of interaction, suggests that GroES may itself possess considerable domain mobility (Landry *et al.,* 1993) or indeed undergo an even more dramatic rearrangement of its 10-kDa subunits within the linear polymer.

We consider it unlikely that the filamentous GroEL–GroES produced by our procedures exists *in vivo,* but it nevertheless represents an unexpected type of linear polymeric complex, from which we have shown that it is possible to obtain further structural information on the interaction of these important macromolecules.

Most EM studies were performed using the Zeiss EM 900, made available by Professor Dr. Albrecht Fischer, Institute of Zoology, University of Mainz. In addition, some work was performed using a Jeol 120EX at the London School of Hygiene and Tropical Medicine (courtesy of Dr. S. Croft) and a Philips EM 400 at the Institute of Physical Chemistry, University of Mainz (courtesy of Dr. I. Voigt-Martin). Grateful thanks are given for the continuing support and encouragement provided by Professor Dr. Jürgen Markl, Institute of Zoology, University of Mainz. R. Z. is supported by a postdoctoral fellowship (Liebig-Stipendium) from the Verband der Chemischen Industrie e.V.

REFERENCES

Azem, A., Kessel, M., and Goloubinoff, P. (1994) Characterization of a functional $GroEL_{14}(GroES_7)_2$ chaperonin hetero-oligomer, *Science* **265,** 653–656.

Braig, K., Otwinowski, Z., Hegde, R., Boisvert, D., Jachimiak, A., Horwich, A., and Sigler, P. B. (1994) The crystal-structure of the bacterial chaperonin GroEL at 2.8 A, *Nature* **371,** 578–586.

Buchner, J., Schmidt, M., Fuchs, M., Jaenicke, R., Rudolph, R., Schmidt, F. X., and Kiefhaber, T. (1991) GroE facilitates refolding of citrate synthetase by suppressing aggregation, *Biochemistry.* **30,** 1586–1591.

Cejka, Z., Gould-Kostka, J., Burns, D., and Kessel, M. (1993) Localization of the binding site of an antibody affecting ATPase activity of the chaperonin cpn60 from *Bordetella pertussis, J. Struct. Biol.* **111,** 34–38.

Chandrasekhar, G. N., Tilly, K., Woolford, C., Hendrix, R., and Georgopoulos, C. (1986) Purification and properties of the GroES morphogenic protein of *Escherichia coli, J. Biol. Chem.* **261,** 12414–12419.

Chen, S., Roseman, A. M., Hunter, A. S., Wood, S. P., Burston, S. G., Ranson, N. A., Clarke, A. R., and Saibil, H. R. (1994) Location of a folding protein and shape changes in GroEL–GroES complexes imaged by cryo-electron microscopy, *Nature* **371,** 261–264.

Couture-Tosi, E., Tapon-Bretaudiere, J., Pochon, M., Bros, A., and Delain, E. (1986) Ultrastructural and anti-proteinase activity modifications of human α-macroglobulin induced by zinc and other divalent cations, *Eur. J. Cell Biol.* **42,** 359–364.

Fenton, W., Kashi, Y., Furtak, K., and Horwich, A. N. (1994) Residues in chaperonin GroEL required for polypeptide binding, *Nature* **371,** 614–619.

Frey, T. G. (1978) The structures of glutamine synthetase and cytochrome c oxidase—Studies by electron microscopy and image analysis, *in* Ninth International Congress on Electron Microscopy, Vol. III, Toronto, pp. 107–119.

Gebauer, W., Harris, J. R., Heid, H., Süling, M., Hillenbrand, R., Söhngen, S., Wegener-Sträke, A., and Markl, J. (1994) Quaternary structure, subunits and domain patterns of two discrete forms of keyhole limpet hemocyanin: KLH1 and KLH2, *Zoology* **98,** 51–68.

Gething, M. J., and Sambrook, J. (1992) Protein folding in the cell, *Nature* **355,** 33–45.

Goloubinoff, P., Christeller, J. T., Gatenby, A. A., and Lorimer, G. H. (1989) Reconstitution of active dimeric ribulose biphosphate carboxylase from an unfolded state depends on two chaperonin proteins and Mg-ATP, *Nature* **342,** 884–889.

Harris, J. R., and Horne, R. W. (1991) Negative staining, *in* Harris, J. R. (Ed.), Electron Microscopy in Biology, pp. 203–238, IRL Press at Oxford Univ. Press, Oxford.

Harris, J. R., Gebauer, W., and Markl, J. (1993) Immunoelectron microscopy of hemocyanin from the keyhold limpet (*Megathura crenulata*): A parallel subunit model, *J. Struct. Biol.* **111,** 96–104.

Harris, J. R., and Horne, R. W. (1994) Negative staining: A brief assessment of current technical benefits, limitations and future possibilities, *Micron* **25,** 5–13.

Harris, J. R., Plückthun, A., and Zahn, R. (1994) Transmission electron microscopy of GroEL, GroES and the symmetrical GroEL/ES complex, *J. Struct. Biol.* **112,** 216–230.

Harris, J. R., Gebauer, W., Söhngen, S. M., and Markl, J. (1995) Keyhold limpet hemocyanin (KLH): Purification of intact KLH1 through selective dissociation of KLH2, *Micron* **26,** 25–33.

Hendrick, J. P., and Hartl, F.-U. (1993) Molecular chaperone functions of heat-shock proteins, *Annu. Rev. Biochem.* **62,** 349–384.

Horne, R. W., and Pasquali-Ronchetti, I. (1974) A negative staining-carbon film technique for studying viruses in the electron microscopy. I. Preparative procedure for examining icosahedral and filamentous viruses, *J. Ultrastruct. Res.* **47,** 361–383.

Hovmöller, S. (1992) CRISP: Crystallographic image processing on a personal computer, *Ultramicroscopy* **41,** 121–135.

Ishii, N., Tagushi, H., Sumi, M., and Yoshgida, M. (1992) Structure of holo-chaperonin studied with electron microscopy, *FEBS Lett.* **299,** 169–174.

Josephs, R., and Borisy, G. (1972) Self-assembly of glutamic dehydrogenase in ordered superstructures: Multichain tubes formed by association of single molecules, *J. Mol. Biol.* **65,** 127–155.

Kiselev, N. A., Shpitzberg, C. L., and Vainshtein, B. K. (1967) Crystallization of catalase in the form of tubes with monomolecular walls, *J. Mol. Biol.* **25,** 433–441.

Laminet, A. A., Ziegelhoffer, T., Georgopoulos, C., and Plückthun, A. (1990) The *Escherichia coli* heat shock proteins GroEL and GoES modulate the folding of the β-lactamase precursor, *EMBO J.* **9,** 2315–2319.

Landry, S. J. Zeilstra-Ryalls, J., Fayet, O., Georgopoulos, C., and Gierash, L. M. (1993) Characterization of a functionally important mobile domain of GroES, *Nature* **364,** 255–258.

Langer, T., Pfeifer, G., Martin, J., Baumeister, W., and Hartl, F.-U. (1992) Chaperonin-mediated protein folding: GroES binds to one end of the GroEL cylinder, which accommodates the protein substrate within its cavity, *EMBO J.* **11,** 4757–6765.

Lorca, O., Marco, S., Carrascosa, J. L., and Valpuesta, J. M. (1994) The formation of symmetrical GroEL–GroES complexes in the presence of ATP, *FEBS Lett.* **345,** 181–186.

McDade, W. A., and Josephs, R. (1993) On the formation and crystallization of sickle hemoglobin macrofibers, *J. Struct. Biol.* **110,** 90–97.

Martin, J., Mayhew, M., Langer, T., and Hartl, F.-U. (1993) The reaction cycle of GroEL and GroES in chaperonin-assisted protein folding, *Nature* **366,** 228–233.

Martin, J., Goldie, K. N., Engel, A., and Hartl, F. U. (1994) Topology of the morphological domains of the chaperonin GroEL visualised by immuno-electron microscopy, *Biol. Chem. Hoppe-Seyler* **375,** 635–639.

Mellema, J. E., and Klug, A. (1972) Quaternary structure of gastropod haemocyanin, *Nature* **239,** 146–150.

Munn, E. A. (1972) Structure of oligomeric and polymeric forms of ox liver glutamate dehydrogenase examined by electron microscopy, *Biochim. Biophys. Acta* **285,** 301–313.

Robinson, C. V., Gross, M., Eyles, S. J., Ewbank, J. J., Mayhew, M., Hartl, F.-U., Dobson, C. M., and Radford, S. E. (1994) Conformation of GroEL-bound α-lactalbumin probed by mass spectrometry, *Nature* **372,** 646–651.

Saibil, H. R., Zeng, D., Wood, S. P., and auf der Maurer, A. (1991) Binding of chaperonins, *Nature* **353,** 25–26.

Saibil, H. R., Zheng, D., Roseman, A. M., Hunter, A. M., Watson, G. M. F., Chen, S., auf der Maurer, A., O'Hara, B. P., Wood, S. P., Mann, N. H., Barnett, L. K., and Ellis, R. J. (1993) ATP induces large quaternary rearrangements in a cage-like chaperonin structure, *Curr. Biol.* **3,** 265–273.

Schmidt, M., Rutkat, K., Rachel, R., Pfeifer, G., Jaenicke R., Viitanen, P., Lorimer, G., and Buchner, J. (1994) Symmetric complexes of GroE chaperonins as a part of the functional cycle, *Science* **265,** 656–659.

Schnyder, T., Cyrklaff, M., Fuchs, K., and Walliman, T. (1994) Crystallization of mitochondrial creatine kinase on negatively charged lipid layers, *J. Struct. Biol.* **112,** 136–147.

Stewart, M. (1986) Computer image processing of electron micrographs of biological structures with helical symmetry, *J. Electron Microsc. Tech.* **9,** 325–358.

Todd, M. J., Viitanen, P. V., and Lorimer, G. H. (1993) Hydrolysis of adenosine 5′-triphosphate by *Escherichia coli* GroEL: Effects of GroES and potassium ion, *Biochemistry* **32,** 8560–8567.

Todd, M. J., Viitanen, P. V., and Lorimer, G. H. (1994) Dynamics of the chaperonin ATPase cycle: Implications for facilitated protein folding, *Science* **265,** 659–666.

Viitanen, P. V., Lorimer, G. H., Seetharam, R., Gupta, R. S., Oppenheim, J., Thomas, J. O., and Cowan, N. J. (1992) Mamma-

lian mitochondrial chaperonin 60 functions as a single toroidal ring, *J. Biol. Chem.* **267,** 695–698.

Wrigley, N. G. (1968) The lattice spacing of crystalline catalase as an internal standard of length in electron microscopy, *J. Ultrastruct. Res.* **24,** 454–464.

Zahn, R. (1994). Doctoral thesis, University of Munchen, Germany, p. 56.

Zahn, R., and Plückthun, A. (1992) GroE prevents the accumulation of early folding intermediates of pre-β-lactamase without changing the folding pathway, *Biochemistry* **31,** 3249–3255.

Zahn, R., Harris, J. R., Pfeifer, G., Plückthun, A., and Baumeister, W. (1993) Two-dimensional crystals of the molecular chaperone GroEL reveal structural plasticity, *J. Mol. Biol.* **229,** 579–584.

Zahn, R., Spitzfaden, C., Ottiger, M., Wuthrich, K., and Plückthun, A. (1994a) Destabilization of the complete protein secondary structure on binding to the chaperone GroEL, *Nature* **368,** 261–265.

Zahn, R., and Plückthun, A. (1994) Thermodynamic partitioning model for hydrophobic binding of polypeptides by GroEL. II. GroEL recognizes thermally unfolded mature β-lactamase, *J. Mol. Biol.* **242,** 165–174.

Zahn, R., Axmann, S. E., Rucknagel, K.-P., Jaeger, E., Laminet, A. A., and Plückthun, A. (1994b) Thermodynamic partitioning model for hydrophobic binding of polypeptides by GroEL. I. GroEL recognizes the signal sequence of β-lactamase precursor, *J. Mol. Biol.* **242,** 150–164.

Zwickl, P., Pfeifer, G., Lottspeich, F., Köpp, F., Dahlmann, B., and Baumeister, W. (1990) Electron microscopy and image analysis reveal common principles of organization in two large protein complexes: groEL-type proteins and proteasomes, *J. Struct. Biol.* **103,** 197–203.